DOE/ER/41014-02-N97

TWO-PION EXCHANGE NUCLEON-NUCLEON POTENTIAL: MODEL INDEPENDENT FEATURES

Manoel R. Robilotta*and Carlos A. da Rocha†
University of Washington, Department of Physics, Box 351560, Seattle, Washington 98195-1560
(November 1996)

A chiral pion-nucleon amplitude supplemented by the HJS subthreshold coefficients is used to calculate the the long range part of the two-pion exchange nucleon-nucleon potential. In our expressions the HJS coefficients factor out, allowing a clear identification of the origin of the various contributions. A discussion of the configuration space behaviour of the loop integrals that determine the potential is presented, with emphasis on cancellations associated with chiral symmetry. The profile function for the scalar-isoscalar component of the potential is produced and shown to disagree with those of several semi-phenomenological potentials.

I. INTRODUCTION

Nowadays there are several semi-phenomenological NN potentials that may be considered as realistic because they provide good descriptions of cross sections, scattering amplitudes and phase shifts. Nevertheless, it is possible to notice important discrepancies when one compares directly their configuration space profile functions. Of course, this situation is consistent with the venerable inverse scattering problem, whereby there are always many potentials that can explain a given set of observables. Therefore one must look elsewhere in order to assess the merits of the various possible models.

In the case of NN interactions, there is a rather rich relationship between the potential and observables, involving several spin and isospin channels and different spatial regions. On the other hand, as all modern models represent the long range interaction by means of the one pion exchange potential (OPEP), one must go to inner regions in order to unravel the discrepancies among the various approaches.

Models vary widely in the way they treat the non-OPEP part of the interaction and, in the literature, one finds potentials constructed by means of dispersion relations, field theory or just based on common sense guesses. In all cases, parameters are used which either reflect knowledge about other physical processes or are adjusted ad hoc. This leaves a wide space for personal whim and indicates the need of information with little model dependence about the inner part of the nuclear force. In the case of NN interactions, the complexity of the relevant physical processes increases very rapidly as the internucleon distance decreases and hence the best process for yielding information with little model dependence is the tail of the two-pion exchange potential ($TPEP$).

This problem has a long history. More than thirty years ago, Cottingham and Vinh Mau began a research program based on the idea that the $TPEP$ is related to the pion–nucleon (πN) amplitude [1]. It lead to the construction of the Paris potential [2,3], where the intermediate part of the force is obtained from empirical πN information treated by means of dispersion relations. This procedure minimizes the number of unnecessary hypotheses and hence yields results which can be considered as model independent. Another important contribution was made by Brown and Durso [4] who stressed, in the early seventies, that chiral symmetry has a main role in the description of the intermediate πN amplitude.

In the last four years the interest in applications of chiral symmetry to nuclear problems was renewed and several authors have reconsidered the construction of the $TPEP$. At first, only systems containing pions and nucleons were studied, by means of non-linear lagrangians based on either PS or PV pion-nucleon couplings [5,6,7,8,9]. Nowadays, the evaluation of this part of the potential in the framework of chiral symmetry has no important ambiguities and is quite well understood. This minimal $TPEP$ fulfills the expectations from chiral symmetry and, in particular, reproduces at the nuclear level the well known cancellations of the intermediate πN amplitude [10,11]. On the other hand, it fails to yield the qualitative features of the medium range scalar-isoscalar NN attraction [8,12]. This happens because a system containing just pions and nucleons cannot explain the experimental πN scattering data [13] and one needs other degrees of freedom, especially those associated with the delta and the πN σ-term. The former possibility was considered by Ordóñez, Ray and Van Kolck [14,15], and shown to improve the predictive power of chiral cancellations but, in their work they did not regard closely the

*Permanent address: Instituto de Física, Universidade de São Paulo, C.P. 66318, 05389-970 São Paulo, SP, Brazil. Electronic address: robilotta@if.usp.br
†Fellow from CNPq Brazilian Agency. Electronic address: carocha@phys.washington.edu

experimental features of the intermediate πN amplitude.

Empirical information concerning the intermediate πN process may be introduced into the $TPEP$ in a model independent way, with the help of the Höhler, Jacob and Strauss (HJS) subthreshold coefficients [13,16]. This kind of approach has already been extensively adopted in other problems. For instance, Tarrach and M.Ericson used it in their study of the relationship between nucleon polarizability and nuclear Van der Waals forces [17]. In the case of three-body forces, it was employed in the construction of both model independent and model dependent two-pion exchange potentials [18,19,20]. Using the same strategy, we have recently shown that the knowledge of the πN amplitude, constrained by both chiral symmetry and experimental information in the form of the HJS coefficients, provides a unambiguous and model independent determination of the long range part of the two-pion exchange NN potential [21]. There we restricted ourselves to the general formulation of the problem and to the identification of the leading scalar-isoscalar potential. In the present work we explore the numerical consequences of the expressions derived in that paper and compare them with some existing potentials.

Our presentation is divided as follows: in Sec. II, we briefly summarize the derivation of the potential and recollect the main formulae for the sake of self-consistency, leaving details to Appendices A, B, and C. In Sec. III we discuss the main features of the loop integrals that determine the potential, emphasizing in the approximations associated with chiral symmetry. In Sec. IV we relate our theoretical expressions with those of other authors and in Sec. V, results are compared with existing phenomenological potentials. Finally, in Sec. VI we present our conclusions.

II. TWO-PION EXCHANGE POTENTIAL

The construction of the $\pi\pi EP$ begins with the evaluation of the amplitude for on-shell NN scattering due to the exchange of two pions. In order to avoid double counting, we must subtract the term corresponding to the iterated OPEP and, on the centre of mass of the NN system, the resulting amplitude is already the desired potential in momentum space. As it depends strongly on the momentum transferred $\mathbf{\Delta}$ and little on the nucleon energy E, we denote it by $T(\mathbf{\Delta})^*$.

In this work we are interested in the central, spin-spin, spin-orbit and tensor components of the configuration space potential, which may be written in terms of local profile functions [22]. They are related with the appropriate amplitudes in momentum space by

$$V(r) = -\Big(\frac{\mu}{2m}\Big)^2 \frac{\mu}{4\pi} \int \frac{d^3\mathbf{\Delta}}{(2\pi)^3}\, e^{-i\mathbf{\Delta}\cdot r} \left[\left(\frac{4\pi}{\mu^3}\right) T(\mathbf{\Delta})\right] . \tag{1}$$

In general, there are many processes that contribute to the $TPEP$. However, for large distances, the potential is dominated by the low energy amplitude for πN scattering on each nucleon. When the external nucleons are on-shell, the amplitude for the process $\pi^a(k)N(p) \to \pi^b(k')N(p')$ is written as

$$F = F^+\,\delta_{ab} + F^-\, i\,\epsilon_{bac}\,\tau_c \ , \tag{2}$$

where

$$F^\pm = \overline{u}\left(A^\pm + \frac{\not k + \not k'}{2}\, B^\pm\right) u \ . \tag{3}$$

The functions $A^\pm$ and $B^\pm$ depend on the variables

$$t = (p-p')^2 \quad \text{and} \quad \nu = \frac{(p+p')\cdot(k+k')}{4m} \tag{4}$$

or, alternatively, on

$$s = (p+k)^2 \quad \text{and} \quad u = (p-k')^2 \ . \tag{5}$$

When the pions are off-shell, they may also depend on k^2 and k'^2. However, as discussed in Ref. [21], off-shell pionic effects have short range and do not contribute to the asymptotic amplitudes. At low energies, $A^\pm$ and $B^\pm$ may be written as a sum of chiral contributions from the pure pion-nucleon sector, supplemented by a series in the variables ν and t [13], as follows:

$$A^+ = \frac{g^2}{m} + \sum a^+_{mn}\,\nu^{2m}\,t^n \quad , \tag{6}$$

$$B^+ = -\frac{g^2}{s-m^2} + \frac{g^2}{u-m^2} + \sum b^+_{mn}\,\nu^{(2m+1)}\,t^n \quad , \tag{7}$$

$$A^- = \sum a^-_{mn}\,\nu^{(2m+1)}\,t^n \quad , \tag{8}$$

$$B^- = -\frac{g^2}{s-m^2} - \frac{g^2}{u-m^2} + \sum b^-_{mn}\,\nu^{2m}\,t^n \quad . \tag{9}$$

In these expressions, the nucleon contributions were calculated using a non-linear pseudoscalar (PS) πN coupling [21] and, in writing A^+, we have made explicit the factor (g^2/m), associated with chiral symmetry. This amounts to just a redefinition of the usual a^+_{00}, given in Refs. [13,16]. On the other hand, the use of a pseudo vector (PV) πN coupling would imply also a small redefinition of b^-_{00}. It is very important to note, however, that the values of the sub-amplitudes $A^\pm$ and $B^\pm$ are not at

*The final relativistic expression for the amplitude depends also on powers of $\vec{z} = \vec{p}\,' + \vec{p}$, which yield "non-local" terms. We expand the amplitude in powers of $\vec{z}/m$ and keep just the first term, which gives the spin-orbit force.

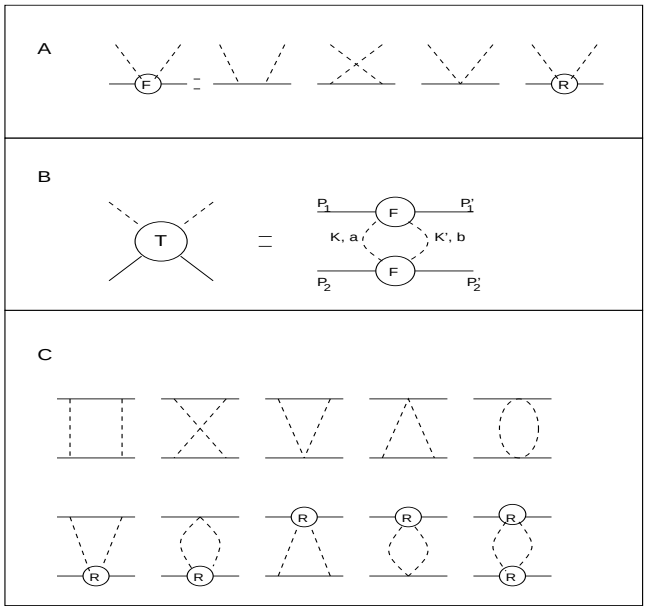

FIG. 1. *A) diagrams contributing to the low-energy πN amplitude, where R represents the processes associated with the HJS coefficients; b) the two-pion exchange amplitude; c) contributions to the two-pion exchange amplitude from the purely pionic sector (top) and from processes involving the HJS coefficients (bottom).*

all influenced by this kind of choice and hence are completely model independent. In the sequence, the terms in these expressions associated with the HJS coefficients will be denoted by $A_R^{\pm}$ and $B_R^{\pm}$, the subscript R standing for "remainder", as indicated in Fig. 1(A).

The evaluation of the diagrams of Fig. 1(B) yields the following general form for T

$$T = -\frac{i}{2}\int \frac{d^4Q}{(2\pi)^4}\,\frac{1}{k^2-\mu^2}\,\frac{1}{k'^2-\mu^2} \times \left[3F^{+(1)}\,F^{+(2)} + 2\boldsymbol{\tau}^{(1)}\cdot\boldsymbol{\tau}^{(2)}\,F^{-(1)}\,F^{-(2)}\right] \qquad (10)$$

where the $F^{(i)}$ are given in Eq. (2) and the factor $\frac{1}{2}$ accounts for the symmetry under the exchange of the intermediate pions. The pion mass is represented by μ and the integration variable Q is defined as

$$Q \equiv \frac{1}{2}\,(k+k')\ . \qquad (11)$$

In the sequence, we will also need the variables

$$W \equiv p_1 + p_2 = p_1' + p_2'\ , \qquad (12)$$

$$\Delta \equiv k' - k = p_1' - p_1 = p_2 - p_2'\ , \qquad (13)$$

$$z \equiv \frac{1}{2}\,[(p_1+p_1') - (p_2+p_2')]\,, \qquad (14)$$

$$V_1 \equiv \frac{1}{2m}\,(W+z)\ , \qquad (15)$$

$$V_2 \equiv \frac{1}{2m}\,(W-z). \qquad (16)$$

The evaluation of the diagrams of Fig. 1(C) produces

$$T = -i\,(2m)^2\,\frac{1}{2}\int\frac{d^4Q}{(2\pi)^4} \times \frac{1}{\left[\left(Q-\frac{1}{2}\,\Delta\right)^2-\mu^2\right]\left[\left(Q+\frac{1}{2}\,\Delta\right)^2-\mu^2\right]} \times\Bigg\{3\left[\left(\frac{g^2}{m}+A_R^+\right)I + \left(-\frac{g^2}{s-m^2}+\frac{g^2}{u-m^2}+B_R^+\right)\not{Q}\right]^{(1)} \times\left[\left(\frac{g^2}{m}+A_R^+\right)I\left(-\frac{g^2}{s-m^2}+\frac{g^2}{u-m^2}+B_R^+\right)\not{Q}\right]^{(2)} + 2\boldsymbol{\tau}^{(1)}\cdot\boldsymbol{\tau}^{(2)}\left[A_R^- I + \left(-\frac{g^2}{s-m^2}-\frac{g^2}{u-m^2}+B_R^-\right)\not{Q}\right]^{(1)} \times\left[A_R^- I + \left(-\frac{g^2}{s-m^2}-\frac{g^2}{u-m^2}+B_R^-\right)\not{Q}\right]^{(2)}\Bigg\}, \qquad (17)$$

where I and $\not{Q}$ are defined with non-relativistic normalizations as

$$I = \frac{1}{2m}\,\overline{u}u\ , \qquad (18)$$

$$\not{Q} = \frac{1}{2m}\,\overline{u}\,Q_\mu\,\gamma^\mu\,u\ . \qquad (19)$$

The integrand also depends implicitly on Q through the variables

$$s_i - m^2 = Q^2 + Q\cdot(W\pm z) - \frac{1}{4}\,\Delta^2\ , \qquad (20)$$

$$u_i - m^2 = Q^2 - Q\cdot(W\pm z) - \frac{1}{4}\,\Delta^2\ , \qquad (21)$$

$$\nu_i = Q\cdot V_i\ . \qquad (22)$$

The integration is symmetric under the operation $Q\to -Q$ and hence nucleon denominators involving s and u yield identical results.

The evaluation of the potential in configuration space requires also an integration over t and the pole structure of Eq. (10) implies that the leading contribution at very large distances comes from the region $t\approx 4\mu^2$ [23], as it is well known. Therefore the form of our results in configuration space becomes more transparent when the contribution of the HJS coefficients is reorganized in terms of the dimensionless variable

$$\theta \equiv \left(\frac{t}{4\mu^2}-1\right). \qquad (23)$$

The amplitudes $A_R^{\pm}$ and $B_R^{\pm}$, associated with the HJS coefficients, are rewritten as

TABLE I. *Values for the dimensionless coefficients of Eqs. (24-27) taken from Ref. [13] and re-stated by Eq. 23.*

(m,n)	$(0,0)$	$(0,1)$	$(0,2)$	$(1,0)$	$(1,1)$	$(2,0)$
α^+_{mn}	3.676 ± 0.138	5.712 ± 0.096	0.576 ± 0.048	4.62	-0.04	1.2 ± 0.02
β^+_{mn}	-2.98 ± 0.10	0.40 ± 0.04	-0.16	-0.68 ± 0.06	0.32 ± 0.04	-0.31 ± 0.02
α^-_{mn}	-10.566 ± 0.212	-1.976 ± 0.144	-0.240 ± 0.032	1.222 ± 0.074	0.208 ± 0.024	-0.33 ± 0.02
β^-_{mn}	9.730 ± 0.172	1.760 ± 0.104	0.40 ± 0.032	0.86 ± 0.07	0.22 ± 0.02	0.25 ± 0.02

$$A_R^+ = \frac{1}{\mu} \sum \alpha^+_{mn} \left(\frac{\nu}{\mu}\right)^{2m} \theta^n \,, \tag{24}$$

$$B_R^+ = \frac{1}{\mu^2} \sum \beta^+_{mn} \left(\frac{\nu}{\mu}\right)^{(2m+1)} \theta^n \,, \tag{25}$$

$$A_R^- = \frac{1}{\mu} \sum \alpha^-_{mn} \left(\frac{\nu}{\mu}\right)^{(2m+1)} \theta^n \,, \tag{26}$$

$$B_R^- = \frac{1}{\mu^2} \sum \beta^-_{mn} \left(\frac{\nu}{\mu}\right)^{2m} \theta^n \,. \tag{27}$$

In defining the coefficients $\alpha^\pm_{mn}$ and $\beta^\pm_{mn}$, we have introduced powers of μ where appropriate so as to make them dimensionless. Their numerical values are given in Tab. I.

Eq. (17) can be naturally decomposed into a piece proportional to g^4, which originates in the pure pion-nucleon sector and a remainder, labelled by R, as in Fig. 1(C). The former was discussed in detail in Refs. [8,12], where numerical expressions were produced, and will no longer be considered here. We concentrate on T_R, which encompasses all the other dynamical effects.

The potential in configuration space may be written as

$$V_R = \left(V^+_{R1} + V^+_{R2} + V^+_{R3} + V^+_{R4} + V^+_{R5} + V^+_{R6} + V^+_{R7} + V^+_{R8}\right) + \boldsymbol{\tau}^{(1)} \cdot \boldsymbol{\tau}^{(2)} \left(V^-_{R1} + V^-_{R2} + V^-_{R3} + V^-_{R4} + V^-_{R5} + V^-_{R6} + V^-_{R7} + V^-_{R8}\right) \tag{28}$$

where the $V^\pm_{R_i}$ are integrals of the form

$$V^\pm_{Ri} = -\left(\frac{\mu}{2m}\right)^2 \frac{\mu}{4\pi} \int \frac{d^3\boldsymbol{\Delta}}{(2\pi)^3} e^{-i\boldsymbol{\Delta}\cdot r} \left[-i \frac{4\pi}{\mu^3} \int \frac{d^4Q}{(2\pi)^4} \, \frac{1}{\left[\left(Q - \frac{1}{2}\,\Delta\right)^2 - \mu^2\right]\left[\left(Q + \frac{1}{2}\,\Delta\right)^2 - \mu^2\right]} \, g^\pm_i \right], \tag{29}$$

and the $g^\pm_i$ are the polynomials in ν/μ and θ given in Appendix A. Thus we obtain the following general result for the $V^\pm_i$

$$V^+_{R1} = -\frac{\mu}{4\pi}\frac{3}{2}\left\{ g^2 \frac{\mu}{m} \alpha^+_{mn} 2 S_{B(2m,n)} + \alpha^+_{k\ell}\alpha^+_{mn} S_{B(2k+2m,\ell+n)} \right\} I^{(1)} I^{(2)}, \tag{30}$$

$$V^+_{R2} = -\frac{\mu}{4\pi}\frac{3}{2}\left\{ g^2 \frac{\mu}{m} \beta^+_{mn} S^\mu_{B(2m+1,n)} + \alpha^+_{k\ell}\beta^+_{mn} S^\mu_{B(2k+2m+1,n)} \right\} I^{(1)} \gamma^{(2)}_\mu, \tag{31}$$

$$V^+_{R4} = -\frac{\mu}{4\pi}\frac{3}{2}\left\{ \beta^+_{k\ell}\beta^+_{mn} S^{\mu\nu}_{B(2k+2m+2,\ell+n)} \right\} \gamma^{(1)}_\mu \gamma^{(2)}_\nu, \tag{32}$$

$$V^-_{R1} = -\frac{\mu}{4\pi}\left\{ \alpha^-_{k\ell}\alpha^-_{mn} S_{B(2k+2m+2,\ell+n)} \right\} I^{(1)} I^{(2)}, \tag{33}$$

$$V^-_{R2} = -\frac{\mu}{4\pi}\left\{ \alpha^-_{k\ell}\beta^-_{mn} S^\mu_{B(2k+2m+1,\ell+n)} \right\} I^{(1)} \gamma^{(2)}_\mu, \tag{34}$$

$$V^-_{R4} = -\frac{\mu}{4\pi}\left\{ \beta^-_{k\ell}\beta^-_{mn} S^{\mu\nu}_{B(2k+2m,\ell+n)} \right\} \gamma^{(1)}_\mu \gamma^{(2)}_\nu, \tag{35}$$

$$V_{R5}^{+}=-\frac{\mu}{4\pi}\frac{3}{2}\frac{\mu}{m}\left\{g^2\alpha_{mn}^{+}S_{T(2m,n)}^{\mu}\right\}\gamma_{\mu}^{(1)}I^{(2)}, \tag{36}$$

$$V_{R7}^{+}=-\frac{\mu}{4\pi}\frac{3}{2}\frac{\mu}{m}\left\{g^2\beta_{mn}^{+}S_{T(2m+1,n)}^{\mu\nu}\right\}\gamma_{\mu}^{(1)}\gamma_{\nu}^{(2)}, \tag{37}$$

$$V_{R5}^{-}=\frac{\mu}{4\pi}\frac{\mu}{m}\left\{g^2\alpha_{mn}^{-}S_{T(2m+1,n)}^{\mu}\right\}\gamma_{\mu}^{(1)}I^{(2)}, \tag{38}$$

$$V_{R7}^{-}=\frac{\mu}{4\pi}\frac{\mu}{m}\left\{g^2\beta_{mn}^{-}S_{T(2m,n)}^{\mu\nu}\right\}\gamma_{\mu}^{(1)}\gamma_{\nu}^{(2)}. \tag{39}$$

The expressions for $V_{R3}^{\pm}$, $V_{R6}^{\pm}$ and $V_{R8}^{\pm}$ are identical respectively to $V_{R2}^{\pm}$, $V_{R5}^{\pm}$ and $V_{R7}^{\pm}$ when the very small differences between ν_1 and ν_2 are neglected. In these results $S_{B(m,n)}$ and $S_{T(m,n)}$ represent integrals of bubble (B) and triangle (T) diagrams, with m and n indicating the powers of (ν/μ) and θ respectively, whose detailed form is presented in appendix B. There, we show that the integrals with one free Lorentz index are proportional to V_i^{μ} whereas those with two indices may be proportional to either $V_i^{\mu}V_i^{\nu}$ or $g^{\mu\nu}$. Therefore we write for both bubble and triangle integrals

$$S_{(m,n)}^{\mu}=V_i^{\mu}S_{(m,n)}^{V}, \tag{40}$$

$$S_{(m,n)}^{\mu\nu}=V_i^{\mu}V_i^{\nu}S_{(m,n)}^{VV}+g^{\mu\nu}S_{(m,n)}^{g}. \tag{41}$$

Using the approximations described in Appendix B and the Dirac equation as in Eq.(B1), we obtain

$$V_{R1}^{+}+V_{R5}^{+}+V_{R6}^{+}=-\frac{\mu}{4\pi}\frac{3}{2}\left\{g^2\frac{\mu}{m}\alpha_{mn}^{+}\left[2S_{B(2m,n)}+2S_{T(2m,n)}^{V}\right]+\alpha_{k\ell}^{+}\alpha_{mn}^{+}S_{B(2k+2m,\ell+n)}\right\}I^{(1)}I^{(2)}, \tag{42}$$

$$\begin{aligned}V_{R2}^{+}+V_{R3}^{+}+V_{R7}^{+}+V_{R8}^{+}=&-\frac{\mu}{4\pi}\frac{3}{2}\left\{g^2\frac{\mu}{m}\beta_{mn}^{+}\left[2S_{B(2m+1,n)}^{V}+2S_{T(2m+1,n)}^{VV}\right]\right.\\&\left.+\alpha_{k\ell}^{+}\beta_{mn}^{+}S_{B(2k+2m+1,n+\ell)}^{V}\right\}I^{(1)}I^{(2)}-\frac{\mu}{4\pi}\frac{3}{2}\left\{g^2\frac{\mu}{m}\beta_{mn}^{+}2S_{T(2m+1,n)}^{g}\right\}\gamma^{(1)}\cdot\gamma^{(2)},\end{aligned} \tag{43}$$

$$V_{R4}^{+}=-\frac{\mu}{4\pi}\frac{3}{2}\left\{\beta_{k\ell}^{+}\beta_{mn}^{+}S_{B(2k+2m+2,\ell+n)}^{VV}\right\}I^{(1)}I^{(2)}-\frac{\mu}{4\pi}\frac{3}{2}\left\{\beta_{k\ell}^{+}\beta_{mn}^{+}S_{B(2k+2m+2,\ell+n)}^{g}\right\}\gamma^{(1)}\cdot\gamma^{(2)}, \tag{44}$$

$$V_{R1}^{-}=-\frac{\mu}{4\pi}\left\{\alpha_{k\ell}^{-}\alpha_{mn}^{-}S_{B(2k+2m+2,\ell+n)}\right\}I^{(1)}I^{(2)}, \tag{45}$$

$$V_{R2}^{-}+V_{R3}^{-}=-\frac{\mu}{4\pi}\left\{\alpha_{k\ell}^{-}\beta_{mn}^{-}2S_{B(2k+2m+1,\ell+n)}^{V}\right\}I^{(1)}I^{(2)}, \tag{46}$$

$$V_{R4}^{-}=-\frac{\mu}{4\pi}\left\{\beta_{k\ell}^{-}\beta_{mn}^{-}S_{B(2k+2m,\ell+n)}^{VV}\right\}I^{(1)}I^{(2)}-\frac{\mu}{4\pi}\left\{\beta_{k\ell}^{-}\beta_{mn}^{-}S_{B(2k+2m,\ell+n)}^{g}\right\}\gamma^{(1)}\cdot\gamma^{(2)}, \tag{47}$$

$$V_{R5}^{-}+V_{R6}^{-}=\frac{\mu}{4\pi}\frac{\mu}{m}\left\{g^2\alpha_{mn}^{-}2S_{T(2m+1,n)}^{V}\right\}I^{(1)}I^{(2)}, \tag{48}$$

$$V_{R7}^{-}+V_{R8}^{-}=\frac{\mu}{4\pi}\frac{\mu}{m}\left\{g^2\beta_{mn}^{-}S_{T(2m,n)}^{VV}\right\}I^{(1)}I^{(2)}+\frac{\mu}{4\pi}\frac{\mu}{m}\left\{g^2\beta_{mn}^{-}S_{T(2m,n)}^{g}\right\}\gamma^{(1)}\cdot\gamma^{(2)}. \tag{49}$$

In configuration space, the spin-dependence of the potential is obtained by means of the non-relativistic results [22]

$$I^{(1)}\,I^{(2)}\;\cong\;1-\frac{\Omega_{S0}}{2m^2}\quad, \tag{50}$$

$$\gamma^{(1)}\cdot\gamma^{(2)}\cong 1+3\frac{\Omega_{S0}}{2m^2}-\frac{\Omega_{SS}}{6m^2}-\frac{\Omega_T}{12m^2}\quad, \tag{51}$$

where

$$\Omega_{S0} = \boldsymbol{L}\cdot\boldsymbol{S}\left(\frac{1}{r}\,\frac{\partial}{\partial r}\right)\ , \tag{52}$$

$$\Omega_{SS} = -\boldsymbol{\sigma}^{(1)}\cdot\boldsymbol{\sigma}^{(2)}\left(\frac{\partial^2}{\partial r^2}+\frac{2}{r}\,\frac{\partial}{\partial r}\right)\ , \tag{53}$$

$$\Omega_T = \hat{S}_{12}\left(\frac{\partial^2}{\partial r^2}\,-\frac{1}{r}\,\frac{\partial}{\partial r}\right)\ , \tag{54}$$

and

$$\hat{S}_{12} = \left(3\boldsymbol{\sigma}^{(1)}\cdot\hat{\mathbf{r}}\,\boldsymbol{\sigma}^{(2)}\cdot\hat{\mathbf{r}}-\boldsymbol{\sigma}^{(1)}\cdot\boldsymbol{\sigma}^{(2)}\right)\ .$$

An interesting feature of the partial contributions to the potential is that they are given by two sets of phenomenological parameters, the πN coupling constant and the HJS coefficients, multiplying structure integrals. These integrals depend on just the pion and nucleon propagators and hence carry very little model dependence. Their main features are discussed in the next section.

III. INTEGRALS AND CHIRAL SYMMETRY

Our expressions for the $TPEP$, given by Eqs. (42-49), contain both bubble and triangle integrals, which depend on the indices m and n, associated respectively with the powers of (ν/μ) and θ, in the HJS expansion. The numerical evaluation of these integrals has shown that there is a marked hierarchy in their spatial behavior and that the functions with $m = n = 0$ prevail at large distances.

In order to provide a feeling for the distance scales of the various effects, in Figs. 2 and 3 we display the ratios $\left[S_{B(m,n)}/S_{B(0,0)}\right]$ and $\left[S^V_{T(m,n)}/S^V_{T(0,0)}\right]$, for some values of m and n, as functions of r.

When considering these figures, it is useful to bear in mind that the $(m,0)$ and $(0,n)$ curves convey different informations. The former series represents the average values of $(\nu/\mu)^m$ and is related to the behavior of the intermediate πN amplitude below threshold. For physical πN scattering, the variable ν is always greater than μ, whereas in the present problem the average values of $(\nu/\mu)^m$ are smaller than 1 for distances beyond 2.5 fm and tend to zero for very large values of r. This is the reason why the construction of the $TPEP$ cannot be based on raw scattering data, but rather, requires the use of dispersion relations in order to transform the πN amplitude to the suitable kinematical region [23]. One has, therefore, a situation similar to the case of three-body forces, as discussed by Murphy and Coon [24], which emphasizes the role of the HJS coefficients.

Regarding the dependence of the integrals on the momentum transferred, one notes that the intermediate πN amplitude in the momentum space is already in the physical $t < 0$ region and does not require any extrapolations. On the other hand, when one goes to configuration space,

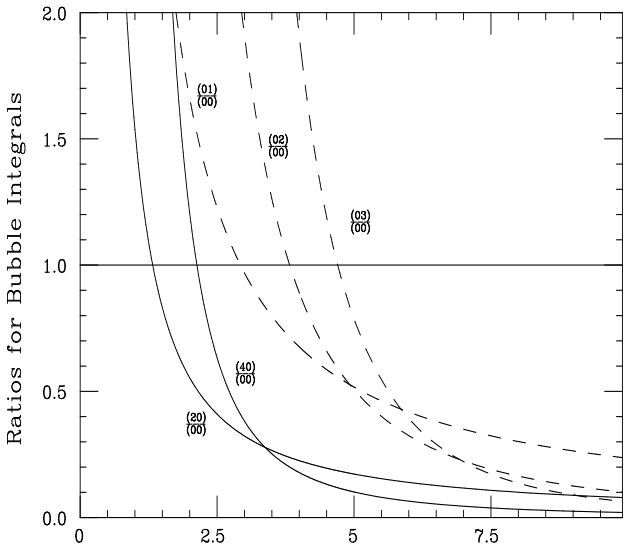

FIG. 2. *Asymptotic behavior of the bubble integrals $S_{B(m,n)}$. The ratios $S_{B(m,0)}/S_{B(0,0)}$ and $S_{B(0,n)}/S_{B(0,0)}$, for some values of m and n are indicated by solid and dashed lines respectively. One sees that the integral $S_{B(0,0)}$ (unity line) is asymptotically dominant.*

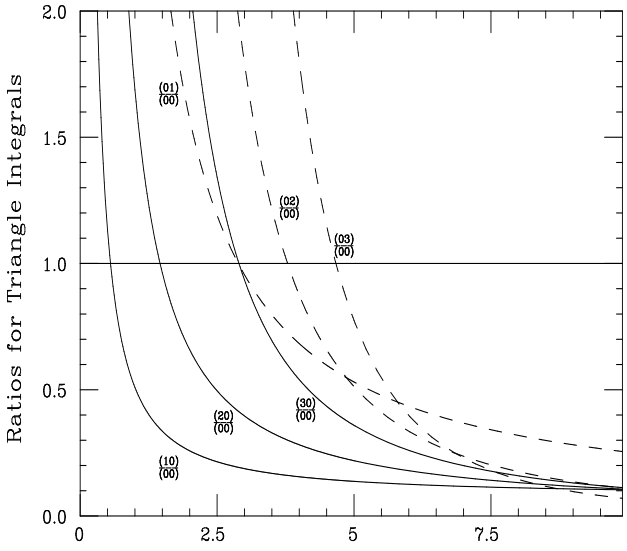

FIG. 3. *Asymptotic behavior of the triangle integrals $S_{T(m,n)}$. The ratios $S_{T(m,0)}/S_{T(0,0)}$ and $S_{T(0,n)}/S_{T(0,0)}$, for some values of m and n are indicated by solid and dashed lines respectively. As in Fig. 2, the integral for $m = n = 0$ is asymptotically dominant.*

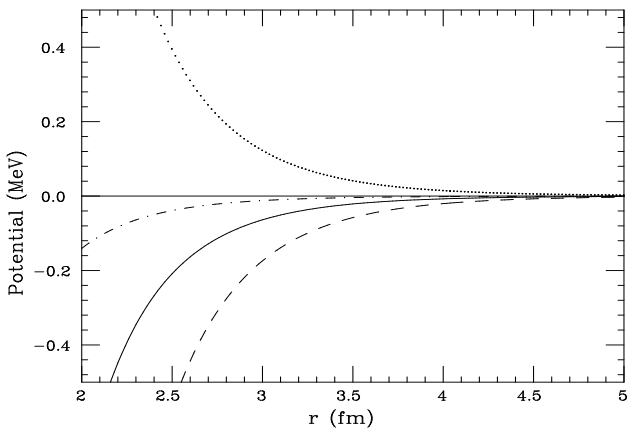

FIG. 4. *Structure of the leading contribution to the central potential, as given by Eq. 55. The continuous line represents the total effect, whereas the dashed, dotted, and dash-dotted lines correspond to the contributions proportional to* $(g^2\mu/m)\alpha^+_{(00)}\, 2S_B$, $(g^2\mu/m)\alpha^+_{(00)}\, 2S_T$, *and* $\left(\alpha^+_{(00)}\right)^2 S_B$ *respectively.*

the Fourier transform picks up values of the amplitude around the point $t = 4\mu^2$. Thus, the r-space potential is not transparent as far as t is concerned and the coherent physical picture only emerges when one uses it in the Schrodinger equation. This is a well known property, which also applies to the OPEP.

The fact that the integrals with $m = n = 0$ dominate at large distances means that the main contribution to the isospin symmetric central potential comes from Eq. (42) and is given by

$$V^+_{R1} + V^+_{R5} + V^+_{R6} = -\frac{\mu}{4\pi}\,\frac{3}{2}\left\{g^2\,\frac{\mu}{m}\,\alpha^+_{00}\right.$$

$$\left.\times\, 2\left[S_{B(0,0)} + S^V_{T(0,0)}\right] + \left(\alpha^+_{00}\right)^2 S_{B(0,0)}\right\} I^{(1)} I^{(2)}. \quad (55)$$

The first term within curly brackets, proportional to g^2, is produced by the triangle and bubble diagrams in Fig. 1(C)-bottom, containing nucleons on one side and HJS amplitudes on the other, whereas the second one is due to the last diagram of Fig. 1(C)-bottom. Inspecting Tab. I one learns that $\left(g^2\mu/m\right)/\alpha^+_{00} \approx 8$, which suggests the first class of diagrams should dominate. On the other hand, the first term is proportional to $\left[S_{B(0,0)} + S^V_{T(0,0)}\right]$ and, as discussed in appendix B, these two integrals have opposite signs and there is a partial cancellation between them. These features of the leading contribution are displayed in Fig. 4, which shows that the first term is indeed dominant.

The cancellation noticed in the leading contributions is not a coincidence. Instead, it represents a deep feature of the problem, which is due to chiral symmetry and also occurs in various other terms of the potential.

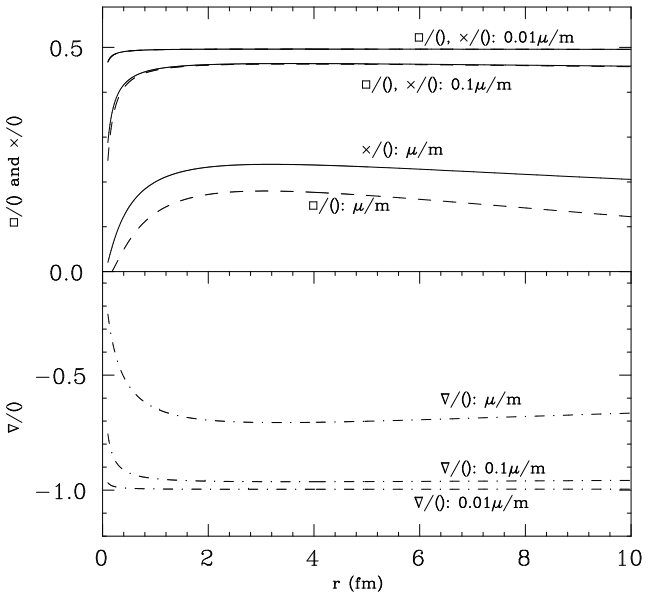

FIG. 5. *Contributions of the box, crossed, and triangle diagrams divided by that of the bubble, in the pure* πN *sector, for the ratios of the pion over the nucleon mass equal to the experimental value* μ/m, *to* $0.1\mu/m$, *and to* $0.01\mu/m$.

In appendix C we have shown that the asymptotic form of $S_{B(0,0)}$ is given by the analytic expression

$$S^{\rm asymp}_{B(0,0)} = \frac{1}{(4\pi)^2}\, 2\sqrt{\pi}\, \frac{e^{-2x}}{x^{5/2}} \left(1 + \frac{3}{16}\frac{1}{x} - \frac{15}{512}\frac{1}{x^2} + \cdots\right) . \quad (56)$$

Its accuracy is 1% up to 1.2 fm. There, we also studied the form of the basic triangle integral $S_{T(0,0)}$ and have demonstrated that $S^{\rm asymp}_{T(0,0)} = -S^{\rm asymp}_{B(0,0)}$ when $(\mu/m) \to 0$. As the integrals with other values of m and n can be obtained from the leading ones, the same relationship holds for them as well. This explains why Figs. 2 and 3 are so similar.

As we have discussed elsewhere [10,11], important cancellations due to chiral symmetry also occur in the pure πN sector. In order to stress this point, we have evaluated the contributions of the diagrams in the top line of Fig. 1(C), denoted respectively by box (□), crossed (⋈), triangle (△) (twice) and bubble (()), for three different values of the ratio μ/m, namely

$$\left(\frac{\mu}{m}\right)^{\rm exp}, \quad \frac{1}{10}\left(\frac{\mu}{m}\right)^{\rm exp}, \quad \text{and} \quad \frac{1}{100}\left(\frac{\mu}{m}\right)^{\rm exp}.$$

In Fig. 5 we display the ratios of the box, crossed and triangle contributions over the bubble result as functions of distance, where it is possible to notice two interesting features. The first is that these ratios tend to become flat as μ/m decreases. The other one is that as $(\mu/m) \to 0$, one obtains the following relations: $\square = 0.5()$, $\bowtie = 0.5()$, and $\triangle = -()$. Thus, for the amplitude in the pure πN

sector, we have $\Box + \bowtie + 2\triangle + () = 0$, a point also remarked by Friar and Coon [7]. This result, when combined with the previous discussion concerning the bottom part of Fig. 1(C), indicates that the two-pion exchange NN potential would vanish if chiral symmetry were exact, because the same would happen with the intermediate πN amplitude. So, all the physics associated with the tail of the intermediate range interaction is due to chiral symmetry breaking.

As a final comment, we would like to point out that in the evaluation of the $TPEP$ there are two different hierarchies that can be used to simplify calculations. One of them concerns the HJS coefficients, which are more important for low powers on ν and t. The other one is associated with the spatial behavior of the integrals as functions of m and n. The combined use of these hierarchies allow many terms to be discarded.

IV. RELATED WORKS

To our knowledge, only Ordóñez, Ray and van Kolck have so far attempted to derive realistic nucleon-nucleon phenomenology in the framework of chiral symmetry [14,15]. The potential obtained by these authors is based on a very general effective Lagrangian, which is approximately invariant under chiral symmetry to a given order in non-relativistic momenta and pion mass. They considered explicitly the degrees of freedom associated with pions, nucleons and deltas, whereas the effects of other interactions were incorporated into parameters arising from contact terms and higher order derivatives. In principle the free parameters in their effective Lagrangian could be obtained from other physical processes, but at present only some of them are known[†]. In their work these parameters were obtained by fitting deuteron properties and NN observables for $j \leq 2$ whereas loop integrals were regularized by means of non-covariant Gaussian cutoffs of the order of the ρ meson mass. Thus they could show that the effective chiral Lagrangian approach is flexible enough for allowing the data to be reproduced with an appropriate choice of dynamical parameters and cutoffs. Comparing their approach to ours, one notes several important differences. For instance, we use dimensional regularization which is well known to preserve the symmetries of the problem and our expressions are quite insensitive to short distance effects. In the work of Ordóñez, Ray and van Kolck, on the other hand, "variations in the cutoff are compensated to some extent by a redefinition of the free parameters in the theory." [15]. Moreover, we use the HJS coefficients as input, which are determined by πN scattering, and therefore our results yield predictions for interactions at large distances or, alternatively, for $j \geq 2$. The test of these predictions will be presented elsewhere.

Another point in the present work that deserves to be discussed concerns the subtraction of the iterated OPEP. In our calculation of the $TPEP$ in the pure nucleonic sector, we have supplemented the results derived by Lomon and Partovi [22] for the pseudoscalar box and crossed box diagrams with bubble and triangle diagrams associated with chiral symmetry [8]. We have also shown that the use of a pseudovector coupling yields exactly the same results and hence that the potential does not depend on how the symmetry is implemented. However, the Partovi and Lomon amplitude include the subtraction of the OPEP by means of the Blankenbecler-Sugar reduction of the relativistic equation and hence our results are also affected by that procedure. This kind of choice should not influence measured quantities, since it amounts to just a selection of the conceptual basis to treat the problem [26]. As discussed by Friar [27] and more recently by Friar and Coon [7], the treatments of the iterated OPEP by Taketani, Machida and Ohnuma [28] and by Brueckner and Watson [29] differ by terms which are energy dependent. However, in our calculation, energy dependent terms can be translated into the variable ν and, in the previous section, we have shown that the $TPEP$ at large distances is dominated by the region where $\nu \approx 0$. Hence our results are not affected by the way the OPEP is defined. Another indication that confirms this fact comes from two recent studies dealing with the relative weights of the various $TPEP$ contributions to NN phase shifts, which have shown that the role of the iterated OPEP is very small for $j \geq 2$ [10,11].

The last comment we would like to make in this section concerns the dynamical significance of the HJS coefficients. It has long been known that a tree model for the intermediate πN amplitude containing nucleons, deltas, rho mesons and an amplitude describing the σ-term can be made consistent with the experimental values of the HJS coefficients by means of a rather conservative choice of masses and coupling constants [13,24,30,31,32]. In general, there are two advantages of employing such a model in a nuclear physics calculation. The first is that it allows one to go beyond the HJS coefficients, specially as far as the the pion off-shell behaviour of the amplitude is concerned. However, as we have discussed above, this kind of off-shell effects are related to short distance interactions and hence are not important for the asymptotic $TPEP$. It is in this sense that we consider our results to be model independent. The second motivation for using a model is that it may provide a dynamical picture involving the various degrees of freedom of the problem and shed light into their relative importance. As we show in the next section, the leading contribution to the scalar-isoscalar potential comes from the coefficient $\alpha_{00}^{+} \equiv \mu(a_{00}^{+} + 4\mu^2 a_{01}^{+} + 16\mu^4 a_{02}^{+})$. As expected, it is attractive and determined mostly by the πN sigma term and by the delta. The former yields $\alpha_{00\Sigma}^{+} = 1.8$ whereas the latter is the outcome of a strong cancellation between

[†]See Ref. [25] for a comprehensive discussion of this point.

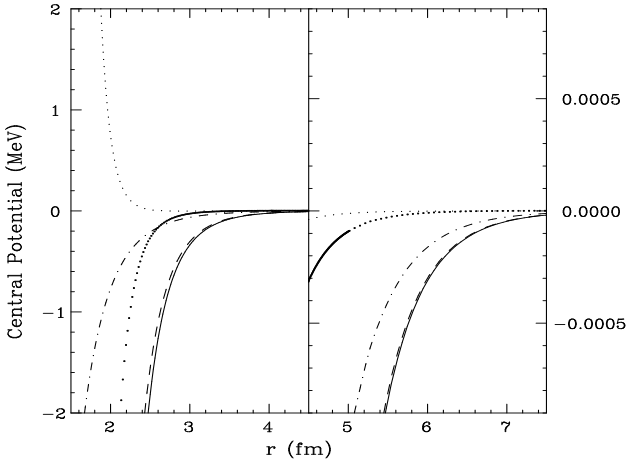

FIG. 6. *Structure of the central potential; the dot-dashed curve represents the leading contribution (Eq. (55)) whereas the dashed, big dotted and small dotted curves correspond to Eqs. (42), (43), and (44) respectively; the solid line represent the full potential.*

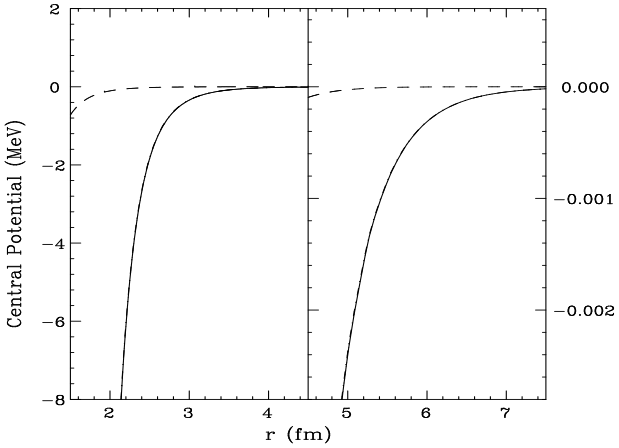

FIG. 7. *Contributions for the total $TPEP$, represented by continuous line; the dashed line comes from the pure πN sector (Fig. 1(C)-top), whereas that associated with other degrees of freedom falls on top of the continuous line and cannot be distinguished from it.*

pole and non-pole contributions $\alpha^{+}_{00\Delta} = (26.5 - 25.2)$ [13]. Thus the delta non-pole term plays a very important role in the interaction, and must be carefully considered in any model aiming at being realistic.

V. RESULTS AND CONCLUSIONS

In this work we have assumed that the $TPEP$ is due to both pure pion-nucleon interactions and processes involving other degrees of freedom, as represented in the top and bottom lines of Fig. 1(C). The former class of processes was evaluated and studied elsewhere [8,11] and hence we here concentrate on the latter.

As discussed in Sec. III, the leading contribution to the potential at large distances is due to the intermediate πN amplitude around the point $\nu = 0$, $t = 4\mu^2$. In order to understand the role played by the other terms, in Fig. 6 we disclose the structure of the scalar-isoscalar potential, given by Eqs. (42-44). There it is possible to see that Eq. (42), associated with the α^{+}_{mn} HJS coefficients, completely dominates the full potential. On the other hand, for moderate distances, there is a clear separation between the curves representing the leading contribution, given by Eq. (55), and the total potential. This indicates that corrections associated with higher powers of ν and t are important there, a feature that could have been anticipated from Figs. 2 and 3.

The total potential, obtained by adding the results of Refs. [8,12] with those of this work, is given in Fig. 7, where it is possible to see that the contribution from the pure nucleon sector is rather small. This information, when combined with those contained in the preceding figures, allows one to conclude that the strength of the scalar-isoscalar attraction at large distances is due mostly to diagrams involving the nucleon on one side and the remaining degrees of freedom on the other.

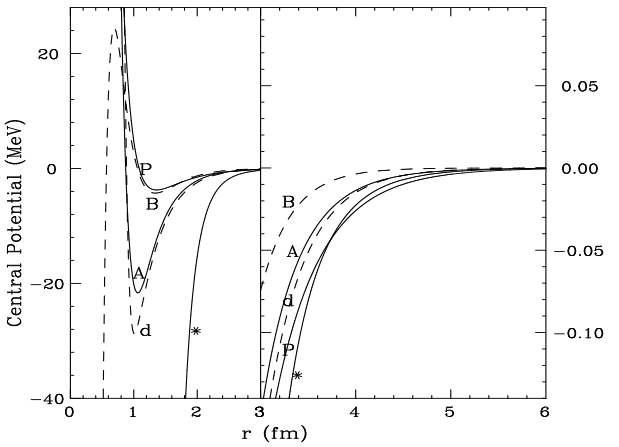

FIG. 8. *Central components of various potentials: parametrized Paris [3] (solid, P), Argonne v14 [33] (solid, A), dTRS [34] (dashed, d), Bonn [35] (dashed, B), and our full potential (solid, *).*

In Fig. 8 we compare our results for the scalar-isoscalar interaction with the corresponding components of some potentials found in the literature: parametrized Paris [3], Argonne v14 [33], dTRS [34], and Bonn [35]. The first thing that should be noted is that all curves but ours bend upwards close to the origin, indicating clearly that the validity of our results is restricted to large distances. Inspecting the medium and long distances regions, it is possible to see that every potential disagrees with all the others. On the other hand, this does not prevent the realistic potentials from reproducing experimental data, something that is possible because there is a compensation arising from the other discrepancies found in the short distance region. It is for this reason that the

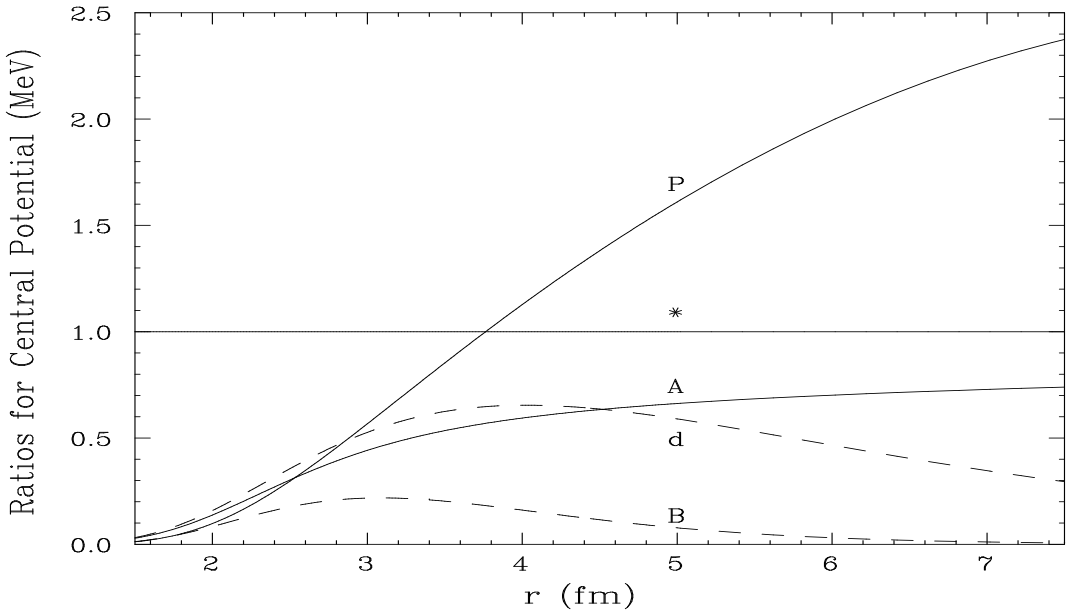

FIG. 9. *Ratio of the central components of some realistic potentials by our full result (solid,*): parametrized Paris [3] (solid, P), Argonne v14 [33] (solid, A), dTRS [34] (dashed, d), and Bonn [35] (dashed, B).*

accurate knowledge of the tail of the potential may yield indirect constraints over its short distance part.

Finally, in Fig. 9 we show the ratios of the realistic potentials by our full potential, where the discrepancies mentioned above appear again, in a different form. An interesting feature of this figure is that the realistic potentials come close together around 2 fm, suggesting that this region is important for reproduction of experimental data. Moreover, all of them show inflections there, indicating that the physics in this region goes beyond the exchange of two uncorrelated pions. In the long distance domain, the r dependence of the Argonne potential is not too different from ours, because it is based on a square OPEP form.

In summary, in this work we have shown that the use of a chiral πN amplitude, supplemented by experimental information, determines uniquely the long-distance features of the scalar-isoscalar component of the NN potential. As it is well known, the kinematical regions relevant to this problem are not directly accessible by experiment and hence empirical information has to be treated by means of dispersion relations before being used as input in the calculations of the force. From a purely mathematical point of view, our results are valid for $r > 2.5$ fm, since in this region one has $\nu < \mu$ and the HJS coefficients may be safely employed. On the other hand, the determination of the dynamical validity of the results is much more difficult, since this requires a comparision with processes involving the mutual interaction of the exchanged pions, something that remains to be done in the framework of chiral symmetry.

In general, a potential involves two complementary ingredients that deserve attention, namely geometry and dynamics. In our calculation, the former is associated with standard bubble and triangle integrals, that determine unambiguously the profile functions in configuration space, whereas dynamics is incorporated into the problem by means of coupling constants and empirical coefficients. Geometry and dynamics decouple in our final expressions and hence they would remain valid even if changes in the values of the dynamical constants may occur in the future. In the case of Fig. 9, such a change would amount to just a modification of the vertical scale, with no appreciable effect on the discrepancies found with phenomenological potentials.

VI. ACKNOWLEDGEMENTS

M.R.R. would like to thank the kind hospitality of Nuclear Theory Group of the Department of Physics of the University of Washington, Seattle, during the performance of this work. This work was partially supported by U.S. Department of Energy. The work of C.A. da Rocha was supported by CNPq, Brazilian Agency.

APPENDIX A: FUNCTIONS $g_i^{\pm}$

We present here the polynomials that enter Eq. (29). The groups of indices $i = 1...4$ and $5...8$ refer, respectively to bubble and triangle diagrams.

$$g_1^+ = 6\frac{m^2}{\mu^2}\left\{g^2\frac{\mu}{m}\alpha^+_{mn}\left[\left(\frac{\nu_1}{\mu}\right)^{2m}+\left(\frac{\nu_2}{\mu}\right)^{2m}\right]\theta^n+\alpha^+_{k\ell}\alpha^+_{mn}\left(\frac{\nu_1}{\mu}\right)^{2k}\left(\frac{\nu_2}{\mu}\right)^{2m}\theta^{(\ell+n)}\right\}I^{(1)}I^{(2)}, \tag{A1}$$

$$g_2^+ = 6\frac{m^2}{\mu^2}\left\{g^2\frac{\mu}{m}\beta^+_{mn}\left(\frac{\nu_2}{\mu}\right)^{(2m+1)}\theta^n+\alpha^+_{k\ell}\beta^+_{mn}\left(\frac{\nu_1}{\mu}\right)^{2k}\left(\frac{\nu_2}{\mu}\right)^{(2m+1)}\theta^{(\ell+n)}\right\}\frac{1}{\mu}I^{(1)}\not{Q}^{(2)}, \tag{A2}$$

$$g_4^+ = 6\frac{m^2}{\mu^2}\left\{\beta^+_{k\ell}\beta^+_{mn}\left(\frac{\nu_1}{\mu}\right)^{(2k+1)}\left(\frac{\nu_2}{\mu}\right)^{(2m+1)}\theta^{(\ell+n)}\right\}\frac{1}{\mu^2}\not{Q}^{(1)}\not{Q}^{(2)}, \tag{A3}$$

$$g_1^- = 4\frac{m^2}{\mu^2}\left\{\alpha^-_{k\ell}\alpha^-_{mn}\left(\frac{\nu_1}{\mu}\right)^{(2k+1)}\left(\frac{\nu_2}{\mu}\right)^{(2m+1)}\theta^{(\ell+n)}\right\}I^{(1)}I^{(2)}, \tag{A4}$$

$$g_2^- = 4\frac{m^2}{\mu^2}\left\{\alpha^-_{k\ell}\beta^-_{mn}\left(\frac{\nu_1}{\mu}\right)^{(2k+1)}\left(\frac{\nu_2}{\mu}\right)^{2m}\theta^{(\ell+n)}\right\}\frac{1}{\mu}I^{(1)}\not{Q}^{(2)}, \tag{A5}$$

$$g_4^- = 4\frac{m^2}{\mu^2}\left\{\beta^-_{k\ell}\beta^-_{mn}\left(\frac{\nu_1}{\mu}\right)^{2k}\left(\frac{\nu_2}{\mu}\right)^{2m}\theta^{(\ell+m)}\right\}\frac{1}{\mu^2}\not{Q}^{(1)}\not{Q}^{(2)}, \tag{A6}$$

$$g_5^+ = \frac{2m\mu}{Q^2-2mQ\cdot V_1-\frac{1}{4}\Delta^2}\,6\frac{m}{\mu}\left\{g^2\alpha^+_{mn}\left(\frac{\nu_2}{\mu}\right)^{2m}\theta^n\right\}\frac{1}{\mu}\not{Q}^{(1)}I^{(2)}, \tag{A7}$$

$$g_7^+ = \frac{2m\mu}{Q^2-2mQ\cdot V_1-\frac{1}{4}\Delta^2}\,6\frac{m}{\mu}\left\{g^2\beta^+_{mn}\left(\frac{\nu_2}{\mu}\right)^{(2m+1)}\theta^n\right\}\frac{1}{\mu^2}\not{Q}^{(1)}\not{Q}^{(2)}, \tag{A8}$$

$$g_5^- = \frac{-2m\mu}{Q^2-2mQ\cdot V_1-\frac{1}{4}\Delta^2}\,4\frac{m}{\mu}\left\{g^2\alpha^-_{mn}\left(\frac{\nu_2}{\mu}\right)^{(2m+1)}\theta^n\right\}\frac{1}{\mu}\not{Q}^{(1)}I^{(2)}, \tag{A9}$$

$$g_7^- = \frac{-2m\mu}{Q^2-2mQ\cdot V_1-\frac{1}{4}\Delta^2}\,4\frac{m}{\mu}\left\{g^2\beta^-_{mn}\left(\frac{\nu_2}{\mu}\right)^{2m}\theta^n\right\}\frac{1}{\mu^2}\not{Q}^{(1)}\not{Q}^{(2)} \tag{A10}$$

The expressions for $g_3^{\pm}$, $g_6^{\pm}$ and $g_8^{\pm}$ are obtained respectively from $g_2^{\pm}$, $g_5^{\pm}$ and $g_7^{\pm}$ by exchanging ν_1 and ν_2.

APPENDIX B: INTEGRALS

In this appendix we present the expressions for the integrals $S_{B(m,n)}$ and $S_{T(m,n)}$ that determine the potential given in Sec. II. In many cases, a considerable simplification of the results, with no loss of numerical accuracy, can be achieved due to the fact that one is interested in the asymptotic behaviour of the potential in configuration space. This allows one to ignore contact terms associated with delta-functions or, alternatively, constant terms in momentum space integrals.

In bubble integrals the denominators involve just two pion propagators, whereas there is an extra nucleon propagator for triangles. In both cases, the integrands have the general form of a polynomial in the variables $\frac{\nu_i}{\mu} = \left(\frac{Q}{\mu}\cdot V_i\right)$, where $V_i = \frac{1}{2m}(W \pm z)$. In elastic pion-nucleon scattering at low energies, $\nu = \mu$ at threshold and hence μ is also a

natural unit for the ν_i. In this problem, $W \approx 2m$, $z \approx p$ and hence $V_i \approx 1$. Moreover, using the mass-shell condition for the external nucleons, we obtain

$$\not{V}^{(i)} = I^{(i)}, \tag{B1}$$

$$V_i^2 = 1 - \frac{\Delta^2}{4m^2}, \tag{B2}$$

$$V_1 \cdot V_2 = 1 - \frac{\Delta^2}{4m^2} - \frac{z^2}{2m^2}. \tag{B3}$$

These results show that the differences between ν_1 and ν_2 are of the order of relativistic corrections and therefore may be neglected.

In our expression for the potential, Lorentz tensors proportional to $\Delta's$ always appear contracted to either V_i or γ matrices. The use of the equations of motion imply in the vanishing of these products and hence we do not write them explicitly below. We also make use of the result $\Delta^2 = t = -\mathbf{\Delta}^2$.

When going to configuration space, it is useful to use the following representation for the logarithm

$$\ln\left[1 + \frac{\mathbf{\Delta}^2}{M^2}\right] = -\int_0^1 d\gamma\, \frac{M^2}{\gamma^2}\, \frac{1}{\mathbf{\Delta}^2 + \frac{M^2}{\gamma}}, \tag{B4}$$

1. Bubble integrals in momentum space:

The basic bubble integral is

$$I_B^{\mu\ldots\sigma} = \int \frac{d^4Q}{(2\pi)^4}\, \frac{\frac{Q^\mu}{\mu}\cdots\frac{Q^\sigma}{\mu}}{\left[(Q-\frac{\Delta}{2})^2-\mu^2\right]\left[(Q+\frac{\Delta}{2})^2-\mu^2\right]}. \tag{B5}$$

The symmetry of the integrand makes all integrals with odd powers of Q to vanish.

The simplest case corresponds to

$$I_B = \int \frac{d^4Q}{(2\pi)^4}\, \frac{1}{\left[(Q-\frac{\Delta}{2})^2-\mu^2\right]\left[(Q+\frac{\Delta}{2})^2-\mu^2\right]}. \tag{B6}$$

Using Feynman integration parameters we write

$$I_B = \int_0^1 d\alpha \int \frac{d^4Q}{(2\pi)^4}\, \frac{1}{\left[Q^2 + 2P\cdot Q - M^2\right]^2}, \tag{B7}$$

where

$$P = \left(\alpha - \frac{1}{2}\right)\Delta\ , \tag{B8}$$

$$M^2 = \mu^2 - \frac{1}{4}\Delta^2\ . \tag{B9}$$

Using the technique of dimensional regularization described in [21], the integration over Q yields, after dropping the constant and divergent terms

$$I_B = -\frac{i}{(4\pi)^2}\int_0^1 d\alpha \ln\left[1 + \frac{\mathbf{\Delta}^2}{M_B^2}\right], \tag{B10}$$

where

$$M_B^2 = \frac{\mu^2}{\alpha(1-\alpha)}. \tag{B11}$$

Using Eq. (B4), we obtain

$$I_B = \frac{i}{(4\pi)^2}\int_0^1 d\alpha \int_0^1 d\beta\, \frac{M_B^2}{\beta^2}\, \frac{1}{\mathbf{\Delta}^2 + \frac{M_B^2}{\beta}}. \tag{B12}$$

For the integral $I_B^{\mu\nu}$, the same procedure yields

$$I_B^{\mu\nu} = \frac{1}{2}\, g^{\mu\nu}\frac{i}{(4\pi)^2}\int_0^1 d\alpha \int_0^1 d\beta\, \left(1 - \frac{1}{\beta}\right)\, \frac{M_B^2}{\beta^2}\, \frac{1}{\mathbf{\Delta}^2 + \frac{M_B^2}{\beta}}, \tag{B13}$$

neglecting terms proportional to $\Delta^\mu\Delta^\nu$.

Analogously, for $I_B^{\mu\nu\rho\lambda}$, we have

$$I_B^{\mu\nu\rho\sigma} = \frac{1}{8}\, \left(g^{\mu\nu}g^{\rho\sigma} + g^{\nu\rho}g^{\mu\sigma} + g^{\mu\rho}g^{\nu\sigma}\right)\frac{i}{(4\pi)^2} \times \int_0^1 d\alpha \int_0^1 d\beta\, \left(1 - \frac{1}{\beta}\right)^2\, \frac{M_B^2}{\beta^2}\, \frac{1}{\mathbf{\Delta}^2 + \frac{M_B^2}{\beta}}. \tag{B14}$$

2. Triangle integrals in momentum space:

The triangle integrals have the structure

$$I_T^{\mu\ldots\sigma} = \int \frac{d^4Q}{(2\pi)^4}\, \frac{2m\mu\ \frac{Q^\mu}{\mu}\ldots\frac{Q^\sigma}{\mu}}{\left[Q^2 - 2mV_i\cdot Q - \frac{1}{4}\Delta^2\right]} \times \frac{1}{\left[(Q-\frac{\Delta}{2})^2-\mu^2\right]\left[(Q+\frac{\Delta}{2})^2-\mu^2\right]}. \tag{B15}$$

The basic case is

$$I_T^{\mu} = \int \frac{d^4Q}{(2\pi)^4}\, \frac{2m\mu\ \frac{Q^\mu}{\mu}}{\left[Q^2 - 2mV_i\cdot Q - \frac{1}{4}\Delta^2\right]} \times \frac{1}{\left[(Q-\frac{\Delta}{2})^2-\mu^2\right]\left[(Q+\frac{\Delta}{2})^2-\mu^2\right]}, \tag{B16}$$

which corresponds to

$$I_T^{\mu} = 2\int_0^1 d\alpha(1-\alpha)\ \int_0^1 d\beta \times \int \frac{d^4Q}{(2\pi)^4}\, \frac{2m\mu\ \frac{Q^\mu}{\mu}}{\left[Q^2 + 2P\cdot Q - M^2\right]^3}, \tag{B17}$$

with

$$P = -\frac{1}{2}\left[\alpha - (1-\alpha)\beta\right]\Delta - (1-\alpha)(1-\beta)mV_i, \tag{B18}$$

$$M^2 = \left[\alpha + (1-\alpha)\beta\right]\mu^2 + \left[1 - 2\alpha - 2(1-\alpha)\beta\right]\frac{\Delta^2}{4}. \tag{B19}$$

Integrating over Q, we have

$$I_T^\mu = -V_i^\mu \frac{i}{(4\pi)^2}\left(\frac{m}{\mu}\right)\int_0^1 d\alpha\,\frac{(1-\alpha)}{\alpha}\int_0^1 d\beta\,\frac{1-\beta}{\beta}\,\frac{2m\mu}{\mathbf{\Delta}^2 + M_T^2}, \tag{B20}$$

where

$$M_T^2 = \frac{\left[\alpha + (1-\alpha)\beta\right]\mu^2 + \left[(1-\alpha)(1-\beta)\right]^2 m^2}{\alpha(1-\alpha)\beta}. \tag{B21}$$

Using the same procedure, and neglecting divergent terms, we get

$$\begin{aligned} I_T^{\mu\nu} &= -V_i^\mu V_i^\nu \frac{i}{(4\pi)^2}\left(\frac{m}{\mu}\right)^2 \int_0^1 d\alpha \frac{(1-\alpha)^2}{\alpha}\int_0^1 d\beta \frac{(1-\beta)^2}{\beta}\,\frac{2m\mu}{\mathbf{\Delta}^2 + M_T^2} \\ &+ g^{\mu\nu}\frac{i}{(4\pi)^2}\left(\frac{m}{\mu}\right)\int_0^1 d\alpha(1-\alpha)\int_0^1 d\beta\int_0^1 d\gamma\,\frac{M_T^2}{\gamma^2}\,\frac{1}{\mathbf{\Delta}^2 + \frac{M_T^2}{\gamma}}. \end{aligned} \tag{B22}$$

$$\begin{aligned} I_T^{\mu\nu\rho} &= -V_i^\mu V_i^\nu V_i^\rho \frac{i}{(4\pi)^2}\left(\frac{m}{\mu}\right)^3 \int_0^1 d\alpha \frac{(1-\alpha)^3}{\alpha}\int_0^1 d\beta \frac{(1-\beta)^3}{\beta}\,\frac{2m\mu}{\mathbf{\Delta}^2 + M_T^2} \\ &+ \left(g^{\mu\rho}V_i^\nu + g^{\nu\rho}V_i^\mu + g^{\mu\nu}V_i^\rho\right)\frac{i}{(4\pi)^2}\left(\frac{m}{\mu}\right)^2 \int_0^1 d\alpha(1-\alpha)^2\int_0^1 d\beta(1-\beta)\int_0^1 d\gamma\,\frac{M_T^2}{\gamma^2}\,\frac{1}{\mathbf{\Delta}^2 + \frac{M_T^2}{\gamma}}. \end{aligned} \tag{B23}$$

$$\begin{aligned} I_T^{\mu\nu\rho\sigma} &= -V_i^\mu V_i^\nu V_i^\rho V_i^\sigma \frac{i}{(4\pi)^2}\left(\frac{m}{\mu}\right)^4 \int_0^1 d\alpha \frac{(1-\alpha)^4}{\alpha}\int_0^1 d\beta \frac{(1-\beta)^4}{\beta}\,\frac{2m\mu}{\mathbf{\Delta}^2 + M_T^2} \\ &+ \left(g^{\mu\nu}V_i^\rho V_i^\sigma + g^{\nu\sigma}V_i^\mu V_i^\rho + g^{\rho\sigma}V_i^\mu V_i^\nu + g^{\mu\rho}V_i^\nu V_i^\sigma + g^{\nu\rho}V_i^\mu V_i^\sigma + g^{\mu\sigma}V_i^\rho V_i^\nu\right) \\ &\times \frac{i}{(4\pi)^2}\left(\frac{m}{\mu}\right)^3 \int_0^1 d\alpha(1-\alpha)^3\int_0^1 d\beta(1-\beta)^2\int_0^1 d\gamma\,\frac{M_T^2}{\gamma^2}\,\frac{1}{\mathbf{\Delta}^2 + \frac{M_T^2}{\gamma}} \\ &+ \frac{1}{2}\left(g^{\mu\nu}g^{\rho\sigma} + g^{\nu\rho}g^{\mu\sigma} + g^{\mu\rho}g^{\nu\sigma}\right)\frac{i}{(4\pi)^2}\left(\frac{m}{\mu}\right)\int_0^1 d\alpha\,\alpha(1-\alpha)\int_0^1 d\beta\,\beta M_T^2\int_0^1 d\gamma\,\frac{M_T^2}{\gamma^2}\left(1 - \frac{1}{\gamma}\right)\frac{1}{\mathbf{\Delta}^2 + \frac{M_T^2}{\gamma}}. \end{aligned} \tag{B24}$$

3. Integrals in configuration space:

The configuration space integrals are obtained by Fourier transforming the results given above multiplied by $(-i)$ and by powers of the variable $\theta = \left(\frac{t}{4\mu^2} - 1\right)$. Recalling that $t = -\mathbf{\Delta}^2$, we have the general structure

$$S(r) = -i\frac{4\pi}{\mu^3}\int \frac{d^3\mathbf{\Delta}}{(2\pi)^3}\,e^{-i\mathbf{\Delta}\cdot r}\left(\frac{-\mathbf{\Delta}^2}{4\mu^2} - 1\right)^n \cdots \int_0^1 d\alpha \int_0^1 \cdots \frac{1}{\mathbf{\Delta}^2 + M^2}. \tag{B25}$$

Neglecting contact terms, we obtain

$$S(r) = -i\frac{4\pi}{\mu^3}\int \frac{d^3\mathbf{\Delta}}{(2\pi)^3}\, e^{-i\mathbf{\Delta}\cdot r}\ \cdots$$

$$\times \int_0^1 d\alpha \int_0^1 \cdots \left(\frac{M^2}{4\mu^2}-1\right)^n \frac{1}{\mathbf{\Delta}^2+M^2} \tag{B26}$$

$$= -i\cdots\int_0^1 d\alpha \int_0^1 \cdots \left(\frac{M^2}{4\mu^2}-1\right)^n \frac{1}{\mu^2}\,\frac{e^{-Mr}}{\mu r} \tag{B27}$$

$$= -i\frac{1}{\mu r}\cdots\hat{\Theta}^n \int_0^1 d\alpha \int_0^1 \cdots \frac{1}{\mu^2}\, e^{-Mr}. \tag{B28}$$

where we use the short notation

$$\hat{\Theta}^n = \left(\frac{1}{4\mu^2}\frac{d^2}{dr^2}-1\right)^n. \tag{B29}$$

In general, the integrals that enter Eqs. (30-39) have at most two free Lorentz indices, since the other ones are contracted with powers of the vectors V_i. Therefore integrals with one free Lorentz index are proportional to V_i^μ and those with two indices are proportional to either $V_i^\mu V_i^\nu$ or $g^{\mu\nu}$, motivating the definitions of Eqs. (40,41). In configuration space, the terms originating from the representation of the logarithm have the form

$$S_n^{log}(M) = \int_0^1 dz\ \frac{M^2}{\mu^2 z^2}\ \left(1-\frac{1}{z}\right)^n e^{-\frac{M}{\sqrt{z}}r}, \tag{B30}$$

These integrals can be evaluated explicitly, and we have

$$S_0^{log}(M) = 2\frac{M^2}{\mu^2}\left[\frac{1}{Mr}+\frac{1}{(Mr)^2}\right]e^{-Mr}, \tag{B31}$$

$$S_1^{log}(M) = -4\frac{M^2}{\mu^2}\left[\frac{1}{(Mr)^2}+\frac{3}{(Mr)^3}+\frac{3}{(Mr)^4}\right] \times e^{-Mr}, \tag{B32}$$

$$S_2^{log}(M) = 16\frac{M^2}{\mu^2}\left[\frac{1}{(Mr)^3}+\frac{6}{(Mr)^4}+\frac{15}{(Mr)^5}+\frac{15}{(Mr)^6}\right] \times e^{-Mr}. \tag{B33}$$

For the bubble integrals this procedure yields the following results

$$S_{B(0,n)} = \frac{1}{(4\pi)^2}\frac{1}{\mu r}\hat{\Theta}^n\int_0^1 d\alpha\, S_0^{log}(M_B), \tag{B34}$$

$$S^g_{B(0,n)} = \frac{1}{2}\frac{1}{(4\pi)^2}\frac{1}{\mu r}\hat{\Theta}^n\int_0^1 d\alpha\, S_1^{log}(M_B), \tag{B35}$$

$$S^V_{B(1,n)} = S^g_{B(0,n)}, \tag{B36}$$

$$S_{B(2,n)} = S^g_{B(0,n)}, \tag{B37}$$

$$S^g_{B(2,n)} = \frac{1}{8}\frac{1}{(4\pi)^2}\frac{1}{\mu r}\hat{\Theta}^n\int_0^1 d\alpha\, S_2^{log}(M_B), \tag{B38}$$

$$S^{VV}_{B(2,n)} = 2S^g_{B(2,n)}, \tag{B39}$$

$$S^V_{B(3,n)} = 3S^g_{B(2,n)}, \tag{B40}$$

$$S_{B(4,n)} = 3S^g_{B(2,n)}. \tag{B41}$$

For the triangle integrals, we obtain

$$S^V_{T(0,n)} = -\frac{1}{(4\pi)^2}\frac{1}{\mu r}\,2\left(\frac{m}{\mu}\right)^2\hat{\Theta}^n\int_0^1 d\alpha\frac{(1-\alpha)}{\alpha} \times\int_0^1 d\beta\,\frac{1-\beta}{\beta}\,e^{-M_T r}, \tag{B42}$$

$$S^{VV}_{T(0,n)} = -\frac{1}{(4\pi)^2}\frac{1}{\mu r}2\left(\frac{m}{\mu}\right)^3\hat{\Theta}^n\int_0^1 d\alpha\frac{(1-\alpha)^2}{\alpha} \times\int_0^1 d\beta\frac{(1-\beta)^2}{\beta}\,e^{-M_T r}, \tag{B43}$$

$$S^g_{T(0,n)} = \frac{1}{(4\pi)^2}\frac{1}{\mu r}(\frac{m}{\mu})\,\hat{\Theta}^n\int_0^1 d\alpha(1-\alpha) \times\int_0^1 d\beta\, S_0^{log}(M_T) \tag{B44}$$

$$S^{VV}_{T(1,n)} = -\frac{1}{(4\pi)^2}\frac{1}{\mu r}2\left(\frac{m}{\mu}\right)^4\hat{\Theta}^n\int_0^1 d\alpha\frac{(1-\alpha)^3}{\alpha} \times\int_0^1 d\beta\frac{(1-\beta)^3}{\beta}\,e^{-M_T r}+2S^g_{T(1,n)}, \tag{B45}$$

$$S^g_{T(1,n)} = \frac{1}{(4\pi)^2}\frac{1}{\mu r}\left(\frac{m}{\mu}\right)^2\hat{\Theta}^n\int_0^1 d\alpha(1-\alpha)^2 \times\int_0^1 d\beta(1-\beta)S_0^{log}(M_T), \tag{B46}$$

$$S^{VV}_{T(2,n)} = -\frac{1}{(4\pi)^2}\frac{1}{\mu r}2\left(\frac{m}{\mu}\right)^5\hat{\Theta}^n\int_0^1 d\alpha\frac{(1-\alpha)^4}{\alpha} \times\int_0^1 d\beta\frac{(1-\beta)^4}{\beta}\,e^{-M_T r} + 5S^g_{T(2,n)}+2S^{g'}_{T(2,n)} \tag{B47}$$

$$S^{g}_{T(2,n)} = \frac{1}{(4\pi)^2}\frac{1}{\mu r}\left(\frac{m}{\mu}\right)^3 \hat{\Theta}^n \int_0^1 d\alpha(1-\alpha)^3 \times \int_0^1 d\beta(1-\beta)^2\, S_0^{log}(M_T), \quad \text{(B48)}$$

$$S^{g'}_{T(2,n)} = \frac{1}{(4\pi)^2}\frac{1}{\mu r}\frac{1}{2}\frac{m}{\mu}\,\hat{\Theta}^n \int_0^1 d\alpha\alpha(1-\alpha) \times \int_0^1 d\beta\beta\,\frac{M_T^2}{\mu^2}\, S_1^{log}(M_T). \quad \text{(B49)}$$

$$S^{V}_{T(1,n)} = S^{VV}_{T(0,n)} + S^{g}_{T(0,n)}, \quad \text{(B50)}$$

$$S^{V}_{T(2,n)} = S^{VV}_{T(1,n)} + S^{g}_{T(1,n)}, \quad \text{(B51)}$$

$$S^{V}_{T(3,n)} = S^{VV}_{T(2,n)} + S^{g}_{T(2,n)} + S^{g'}_{T(2,n)}. \quad \text{(B52)}$$

APPENDIX C: ANALYTICAL RESULTS FOR SOME INTEGRALS

In this appendix we present analytic results for the asymptotic bubble and triangle integrals in configuration space needed in this work.

The basic bubble integral is

$$S_{B(0,0)} = \frac{1}{(4\pi)^2}\,\frac{2}{\mu r}\int_0^1 d\alpha\frac{M_B^2}{\mu^2}\left[\frac{1}{M_B r}+\frac{1}{(M_B r)^2}\right]e^{-M_B r}, \quad \text{(C1)}$$

where

$$M_B^2 = \frac{\mu^2}{\alpha(1-\alpha)}. \quad \text{(C2)}$$

Defining a new variable t such that

$$\alpha = \frac{1}{2} + \frac{t\sqrt{2+t^2}}{1+t^2}, \quad \text{(C3)}$$

we have

$$S_{B(0,0)} = \frac{1}{(4\pi)^2}2\sqrt{2}\,\frac{1}{x}\int_0^\infty dt\frac{1}{(1+t^2)^2\sqrt{1+\frac{t^2}{2}}} \times \left[\frac{2(1+t^2)}{x}+\frac{1}{x^2}\right]e^{-2(1+t^2)x}, \quad \text{(C4)}$$

where $x = \mu r$. For large values of x, the integrand is very peaked around $x \approx 0$ and hence we expand the functions in front the exponential in a power series. Keeping the first three terms, we obtain our asymptotic expression

$$S^{asymp}_{B(0,0)} = \frac{1}{(4\pi)^2}2\sqrt{\pi}\,\frac{e^{-2x}}{x^{\frac{5}{2}}}\left(1+\frac{3}{16\,x}-\frac{15}{512\,x^2}+\cdots\right). \quad \text{(C5)}$$

For the triangle case, we have

$$S^{V}_{T(0,0)} = -\frac{1}{(4\pi)^2}\frac{2}{\mu r}\int_0^1 d\alpha\frac{1}{\alpha(1-\alpha)} \times \int_0^{\frac{m}{\mu}(1-\alpha)} ds\,\frac{s}{1-\frac{\mu s}{m\,(1-\alpha)}}\,e^{-M_T\,r}, \quad \text{(C6)}$$

where we have used a new variable $s \equiv (1-\beta)(1-\alpha)\frac{m}{\mu}$. The function M_T^2 is given by eq.(B21) and can be rewritten as

$$M_T^2 = M_B^2\frac{\left[1-\frac{\mu}{m}s+s^2\right]}{1-\frac{\mu s}{m\,(1-\alpha)}}. \quad \text{(C7)}$$

In the limit of $\frac{\mu}{m} \to 0$ we have

$$S^{V}_{T(0,0)} = -\frac{1}{(4\pi)^2}\frac{2}{\mu r}\int_0^1 d\alpha\frac{1}{\alpha(1-\alpha)}\int_1^\infty dy\; y e^{-M_B\,y\,r} \quad \text{(C8)}$$

where $y = \sqrt{1+s^2}$. Performing the y integration and comparing it with Eq. (C1), we find

$$S^{V}_{T(0,0)} = -S_{B(0,0)}\,. \quad \text{(C9)}$$

[1] W.N. Cottingham and R. Vinh Mau, Phys. Rev. 130, 735 (1963); W.N. Cottingham, M. Lacombe, B. Loiseau, J.M. Richard, and R. Vinh Mau, Phys. Rev. D8, 800 (1973).
[2] W.N. Cottingham, M. Lacombe, B. Loiseau, J.M. Richard, and R. Vinh Mau, Phys. Rev. D **8**, 800 (1973).
[3] M. Lacombe, B. Loiseau, J.M. Richard, R. Vinh Mau, J.Coté, P. Pires and R. de Tourreil, Phys. Rev. C **21**, 861 (1980).
[4] G.E. Brown and J.W. Durso, Phys. Lett. B **35**, 120 (1971).
[5] C. Ordóñez and U. Van Kolck, Phys. Lett. B **291**, 459 (1992).
[6] L.S. Celenza, A. Pantziris and C.M. Shakin, Phys. Rev. C **46**, 2213 (1992).
[7] J.L. Friar and S.A. Coon, Phys. Rev. C **49**, 1272 (1994).
[8] C.A. da Rocha and M.R. Robilotta, Phys. Rev.C **49**, 1818 (1994).
[9] M.C. Birse, Phys. Rev. C **49**, 2212 (1994).
[10] J-L. Ballot and M.R. Robilotta, Z. Phys A **355**, 81 (1996).
[11] J-L. Ballot, M.R. Robilotta, and C.A. da Rocha, *hep-ph/9502369*, to be published in Int. J. Mod. Phys. E.
[12] C.A. da Rocha and M.R. Robilotta, Phys. Rev. C **52** 531 (1995).

[13] G. Höhler, group I, vol. 9, subvol. b, part 2 of Landolt-Börnstein Numerical Data and Functional Relationships in Science and Technology, ed. H. Schopper.
[14] C. Ordóñez, L. Ray and U. Van Kolck, Phys. Rev. Lett. **72**, 1982 (1994).
[15] C. Ordóñez, L. Ray and U. Van Kolck, Phys. Rev. C **53**, 2086 (1996).
[16] G. Höhler, H.P. Jacob and R. Strauss, Nucl. Phys. B **39**, 237 (1972); R. Koch and E. Pietarinen, Nucl. Phys. A **336**, 331 (1980).
[17] R. Tarrach and M. Ericson, Nucl. Phys. A **294**, 417 (1978).
[18] S.A. Coon, M.S. Scadron and B.R. Barrett, Nucl. Phys. A **242**, 467 (1975); S.A. Coon, M.S. Scadron, P.C. McNamee, B.R. Barrett, D.W.E. Blatt and B.H.J. McKellar, Nucl. Phys. A **317**, 242 (1979); S.A. Coon and W. Glöckle, Phys. Rev. C **23**, 1790 (1981).
[19] H.T. Coelho, T.K. Das and M.R. Robilotta, Phys. Rev. C **28**, 1812 (1983); M.R. Robilotta and H.T. Coelho, Nucl. Phys. A **460**, 645 (1986).
[20] T. Ueda,T. Sawada, T. Sasakawa and S. Ishikawa, Progr. Theor. Phys. **72**, 860 (1984).
[21] M.R. Robilotta, Nucl. Phys. A **595**, 171 (1995).
[22] M.H. Partovi and E. Lomon, Phys. Rev. D **2**, 1999 (1970).
[23] G.E. Brown and A.D. Jackson, *The Nucleon-Nucleon Interaction*, American Elsevier Pub. Co., New York, (1976).
[24] D.P. Murphy and S.A. Coon, Few Body Sys. **18**, 73 (1995).
[25] V. Bernard, N. Kaiser, and Ulf-G. Meissner, Int. J. Mod. Phys. E **4**, 193 (1995).
[26] B. Desplanques and A. Amghar, Z. Phys. A **344**, 191 (1992); A. Amghar and B. Desplanques, Nucl. Phys. A **585**, 657 (1995).
[27] J.L. Friar, Ann. Phys. (N.Y.) **104**, 380 (1977).
[28] M. Taketani, S. Nakamura, and M. Sasaki, Prog. Theor. Phys. (Kyoto) **6**, 581, (1951).
[29] K.A. Brueckner and K.M. Watson, Phys. Rev. **90**, 699; **92**, 1023 (1953).
[30] M.G. Olson and E.T. Osypowski, Nucl. Phys. B **101**, 13 (1975).
[31] M.D. Scadron and L.R. Thebaud, Phys. Rev. D **9**, 1544 (1974).
[32] A.M.M. Menezes, M.Sc. Thesis, University of São Paulo, 1985 (unpublished).
[33] R.B. Wiringa, R.A. Smith, and T.L. Ainsworth, Phys. Rev. C **29**, 1207 (1984).
[34] R. de Tourreil, B. Rouben, and D.W.L. Sprung, Nucl. Phys. A **242**, 445 (1975).
[35] R. Machleidt, K. Holinde and C. Elster, Phys. Rep. **149**, 1 (1987).